Effect of microstructure of fluorinated acrylic coatings on UV degradation testing

Li-Piin Sung[a],*, Silvia Vicini[b], Derek L. Ho[a], Lotfi Hedhli[c], Christyn Olmstead[c], Kurt A. Wood[c]

[a]*National Institute of Standards and Technology, Gaithersburg, MD 20899, USA*
[b]*Dipartimento di Chimica e Chimica Industriale, University of Genoa, Via Dodecaneso 31, 16146 Genoa, Italy*
[c]*Atofina Chemicals Inc. R&D Center, 900 First Avenue, King of Prussia, PA 19406, USA*

Abstract

This paper presents research results on the relationships between the microstructure and the performance/weatherability of fluoropolymer/acrylic coatings. We studied fluoropolymer/acrylic blends of identical composition, prepared as films using three different methods: 2-stage emulsion polymerization followed by latex film formation; cold-blending (physically mixing) acrylic and fluoropolymer latex dispersions followed by latex film formation; and solution casting using an organic solvent. We investigated the effects of the mixing method, and the level of acrylic in the blend on the microstructure/morphology and on the durability-related physical properties of the fluoropolymer/acrylic films. Small angle neutron scattering was performed to determine the microstructure/morphology of fluoropolymer-rich micro-domains in the coatings prepared using these three methods. The physical properties tested included the glass transition temperature, the crystallinity fraction, and the tensile strength. The mass loss rates observed during UV exposure testing correlate with the final microstructures of the films.
© 2004 Elsevier Ltd. All rights reserved.

1. Introduction

Fluorocarbon polymers have greatly gained in importance as binders for exterior coatings because of their excellent resistance to UV-A and UV-B radiation, as well as to many corrosive chemical agents [1–3]. For example, architectural coatings based on polyvinylidene fluoride (PVDF) resins have performed successfully in 30-year exterior durability testing [1]. Typical PVDF commercial coatings are solvent dispersion coatings, and must be baked at high temperature to achieve a favorable mixing of the chemically inert, semi-crystalline PVDF resin with a miscible acrylic co-resin. It remains a great challenge to use PVDF-based resins in low volatile organic compound (VOC) waterborne formulations which still perform at levels comparable to those achieved in commercial solvent-based coatings.

The durability and appearance of PVDF coatings depend on the final microstructure/morphology that is attained, which in turn depends on the coating application and processing conditions, as well as many formulation details including the state of dispersion of the coating components. To understand the relationship between durability-related physical properties and the microstructure of fluoropolymer coatings, we compared the microstructure and physical properties of fluoropolymer/acrylic blends of identical composition, prepared as films at ambient temperature using three different methods: 2-stage emulsion polymerization followed by latex film formation; cold-blending (physically mixing) acrylic and fluoropolymer latex dispersions followed by latex film formation; and solution casting using an organic solvent.

In this paper, we discuss the effect of the film preparation method on the microstructure/morphology, and on the physical properties of the coating film. We also investigate how the acrylic concentration affects the morphology of the coatings to yield different material properties. Small angle

* Corresponding author.

neutron scattering (SANS) was performed to determine the microstructure/morphology of fluoropolymer-rich micro-domains in the coatings prepared using the three different blending techniques. The physical properties tested included the glass transition temperature, the crystallinity fraction, and the tensile strength. The mass loss due to UV exposure testing was also measured, and is correlated with the final microstructure of the films.

2. Experimental[1]

2.1. Materials

A series of fluoropolymer/acrylic coating films were prepared using three different blending techniques—2-stage emulsion polymerization followed by latex film formation (EP); cold-blending (physically mixing) acrylic and fluoropolymer latex dispersions followed by latex film formation (latex blend or LB); and solution casting using an organic solvent (solution blend or SB).

A low crystallinity copolymer of vinylidene fluoride/hexafluoropropylene (with approximately 75:25 mass ratio) was used as fluoropolymer component, and a methyl methacrylate/butyl acrylate (MMA/BA) copolymer, with a small amount of copolymerized methacrylic acid (MA), was used as the acrylic component. Component glass transition (T_g) values were $-30\,°C$ for the fluoropolymer, and in the $60–90\,°C$ range for the acrylics depending on the system. The two polymer components were experimentally determined to be miscible in the melt phase (above the fluoropolymer crystalline melting point), below a cloud point transition in the $160–200\,°C$ range depending on the component mass ratio [4]. The latex dispersions had particle sizes in the $100–150$ nm range.

The 2-stage EP process generates latex dispersion particles where every particle contains both the fluoropolymer and acrylic components [5]; the structure of the particles can vary between core-shell and homogeneous. For the EP dispersions used in these studies, the morphology is believed to be substantially homogeneous, based on a number of lines of evidence, not reported here, including NMR double resonance experiments. However, the homogeneity is not complete at 70% (by mass) fluoropolymer, since there is some residual fluoropolymer crystallinity in the particles. It is also likely, since the acrylic copolymer is more hydrophilic, that there is some acrylic enrichment at the latex particle surface.

The LB process begins with a physical blend of two pure component latex dispersions (fluoropolymer latex and acrylic latex) of comparable particle size. Thus the initial

degree of polymer mixing is much coarser than for the EP process. For both the LB and EP process, latex film formation is used to make continuous films, using a small amount of coalescent when necessary to achieve 'good' films (i.e. smooth films with at least some mechanical integrity) [6]. The coalescent, which acts as a fugitive plasticizer, ensures sufficient polymer mobility to achieve particle deformation and the interdiffusion of polymer chains across latex particle boundaries. Films were aged at least 1 month prior to testing.

At the other extreme for the degree of initial polymer mixing, the SB process uses an organic solvent to create a true solution blend of the components. In this study, the component resins were dissolved separately in acetone (5% mass fraction) and then the two solutions were mixed according to the desired composition of fluoropolymer/acrylic resins. The final blend films were obtained by evaporating the solvent at room temperature.

Two different mass fraction ratios of fluoropolymer and acrylic (see Table 1) were selected to investigate the effect of the acrylic content of the mixture on the coating properties. The composition of the fluoropolymer/acrylic films is designated as a mass fraction ratio of F/A (fluoropolymer/acrylic), where 'F' is the fluoropolymer component, and 'A' is the acrylic component. The labels of the samples include the method of the preparation and the composition of the mixtures; for example EP70 represents an EP blend with composition of F/A = 70:30.

2.2. Small angle neutron scattering (SANS)

SANS measurements were performed at the NIST Center for Neutron Research using the 30 m SANS instrument with a combination of various wavelengths and a special focusing neutron optics-device [7] to achieve the wide range of size scale from 1 nm to 1 μm. After standard calibrations and taking into account the sample transmission and film thickness, two-dimensional scattering images (see an example in the insert of Fig. 3) were averaged azimuthally to produce a one-dimensional absolute scattered intensity curve as a function of the scattering wave vector q ($q = 4\pi\sin(\theta/2)/\lambda$, where θ is the scattering angle and λ is the wavelength). Since the fluoropolymer has a higher neutron scattering cross-section than the acrylic, the scattered intensity is proportional, to first order, to differences in the fluoropolymer local concentration within the sample. A peak in the scattering profile at scattering wave vector q indicates the existence of a fluoropolymer-rich micro-domains with a characteristic average length $d = 2\pi/q$ [8]. In this way, microstructure/morphology information, such as the dimension of ordered domains or the correlation length of concentration fluctuations, can be determined from the intensity profile. The estimated extended uncertainties ($k=2$) in the SANS data presented in this paper are smaller than the size of symbols in all figures.

---

[1] Certain instruments or materials are identified in this paper in order to adequately specify experimental details. In no case does it imply endorsement by NIST or imply that it is necessarily the best product for the experimental procedure.

Table 1
Composition and related physical properties of samples before and after 315 h of QUV-B treatments

Sample	Initial latex particle size D_w (nm)	T_g (°C)±1 °C (second heating)		ΔH (J/g)±1 J/g (first heating)		Young's modulus E (N/m^2)±10%		Percent strain at break, ± 20%	
		Before	After	Before	After	Before	After	Before	After
EP70	119.8±2.5	−1	8	3	6	0.10	18	370	30
SB70	–	27	–	–	–	4.5	9.3	300	130
EP30	148.5±2.5	24	32	∼0	1	0.11	25	340	20
SB30	–	45	–	–	–	4.8	21	100	15
LB30	–	21 and 55	30	1	4	4.8	22	130	4

2.3. Material properties measurements and UV exposure testing

Physical and mechanical tests of the blend films, including glass transition temperature, crystallinity fraction, latex particle size, and tensile strength were performed on the coatings. To determine the performance and weatherability of the coatings—none of which contained any added UV absorbers or stabilizing agents, UV exposure experiments were also carried out, in conjunction with mass loss measurements (QUV-B unit, with 313 nm maximum UV light and cycles of different humidity and temperature conditions, described in ASTM G53-88 [9] and ASTM D 4587 Condition D [10]). A second controlled experiment reproducing the same cyclic temperature and humidity conditions but with the light turned off was used to distinguish the temperature and humidity effects from the UV-B degradation effect. Detailed information of the measurements is described elsewhere [11,12].

The latex particle sizes were determined using the capillary hydrodynamic fractionation (CHDF 2000, Matec Applied Sciences) technique after diluting the latex with deionized water to approximately 1% mass concentration. Here, D_w is the average size by mass.

The glass transition temperature, T_g, and the fluoropolymer enthalpy of melting, ΔH, were determined from differential scanning calorimeter measurements (TA Instruments Modulated DSC 2920, cycled at 10 °C/min from −140 to +175 °C), using second and first heat measurements, respectively. The ΔH, which is an indirect measure of crystallinity fraction (degree of crystallinity) in the mixture, was obtained from the area of DSC melting curves integrated between +50 and +120 °C.

The mechanical properties including Young's modulus of the films for various samples were measured using an Instron model 4202, with Instron Series IX Automated Materials Testing System software.

3. Results and discussion

In order to compare the performance/durability of the coatings, the mass changes were measured for a period of 2000 h after QUV-B treatments and a controlled temperature-humidity exposure as described previously. The UV-induced mass loss is the quantity presented in Fig. 1. This quantity is the difference between the total percent mass loss observed in the QUV-B, and the percent mass loss observed for the same sample in a controlled temperature–humidity cabinet reproducing the same cyclic temperature and humidity conditions as the QUV chamber. In this way, any mass loss due only to temperature and humidity cycling is distinguished from the mass loss specifically induced by the UV radiation [12]. Here the mass loss is defined as $ML(\%) = [(M_0 - M_t)/M_{0,f}] \times 100$, where M_0 is the mass of the sample (film on panel) before exposure; M_t is the mass of the sample (film on panel) after an exposure time t, and $M_{0,f}$ is the mass of the free film before the exposure.

In recent studies of some waterborne coatings we have observed a rapid mass loss at the beginning of QUV-B exposure, followed by a period of relative stabilization [5]. Therefore, we focused our attention on this exposure period, which has also been reported in the literature as 'accelerated exposure' or 'degradation'. Interestingly, the UV-induced mass loss for both EP blends is less than 2% and reaches 'stabilization' status around 1500 h. However, the UV-B induced mass loss for the LB30 sample is 5% at 2000 h, and the mass loss appears to be continuing at that point.

In addition to measuring the mass loss as a function of exposure time, the gloss retention of the blend films was measured. The gloss measurements reflect the roughening
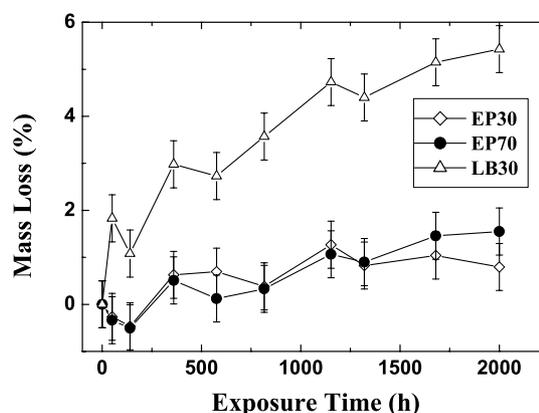

Fig. 1. Coating percent mass loss (ML) as a function of QUV-B cabinet exposure time, which is due directly to the effect of UV radiation (see text for explanation of calculation method).

of the surface after QUV-B exposure. After 2500 h, EP30 blend lost about 5%, while the LB30 lost about 16% of its gloss. Consistent with the mass loss results, the UV resistance of the LB blend is inferior to that of the EP blend.

Table 1 summarizes some thermal and related physical properties of the samples studied, initially and after an initial induction period in the QUV-B unit. In principle, the T_g values of the blends give a measure of the acrylic content of the amorphous phase, since the pure acrylic T_g ($> 60\,°C$) is much higher than the fluoropolymer T_g (about $-30\,°C$). Previous experience in the Atofina laboratory has shown that the Fox equation [13] provides a good estimate of the blend T_g in these kinds of systems. In practice, first heat T_g values above room temperature can be difficult to measure in systems with residual fluoropolymer crystallinity, since fluoropolymer melting peaks from 'cold crystallization' tend to occur at these same temperatures. Fig. 2 shows the DSC curve obtained for the EP70 sample, which illustrates the cold crystallization behavior. To accurately determine first heat T_g values for these systems using DSC, modulated DSC techniques must be used. However, with conventional DSC, glass transitions well below room temperature can be seen. The lack of any apparent first heating low temperature (pure fluoropolymer) T_g, even in the latex blend (LB) cases, suggests that all the systems studied undergo some degree of mixing prior to, or during, film formation. In Table 1 we report second heat T_g values for the various blends. These values give an indication of the degree of spontaneous polymer mixing attainable under conditions of thermal annealing. All the blends studied here exhibited second heat T_gs at intermediate temperatures (in the -1 to $+45\,°C$ range), indicating miscibility of the polymers.

The first heat enthalpy of melting ΔH can provide a complementary measure of the degree of polymer mixing in a blend, since it arises from a pure fluoropolymer phase. Blending with compatible acrylics shifts the equilibrium, reducing the amount of crystallinity per unit of fluoropolymer. In studies of melt blended systems of this type, typically no residual crystallinity is seen once the acrylic level reaches 50% or higher [14]. Higher than expected ΔH values (more crystallinity) indicate fluoropolymer-rich domains in the blend. However, just as with the first heat DSC values, it is difficult in practice to use DSC-ΔH values to achieve more than a rough estimate of crystallinity levels. This is because it can be difficult to unambiguously draw the baseline used in the integration.

Table 1 also lists the T_g and ΔH data after 315 h of QUV-B treatment. Since our main interest is in the performance of the waterborne systems, we only present the results for EP and LB blends for the UV treatments. After the UV treatment, the second heat T_g values increase for all of the blend films. This could be the result of the loss of low molecular mass plasticizing components (one part of the small mass loss which occurs during initial QUV-B exposure is also observed during thermal cycling experiments in the absence of light). The first heat enthalpy of melting data suggests that there may also be some minor increase in the fluoropolymer crystallinity.

The mechanical properties—Young's modulus—of the films for various samples before and after 315 h QUV-B treatment—are also shown in Table 1. Before the treatment, the LB (and SB) blends are much more rigid than the EP samples (i.e. they have higher Young's modulus). This could be explained by a higher homogeneity in the EP
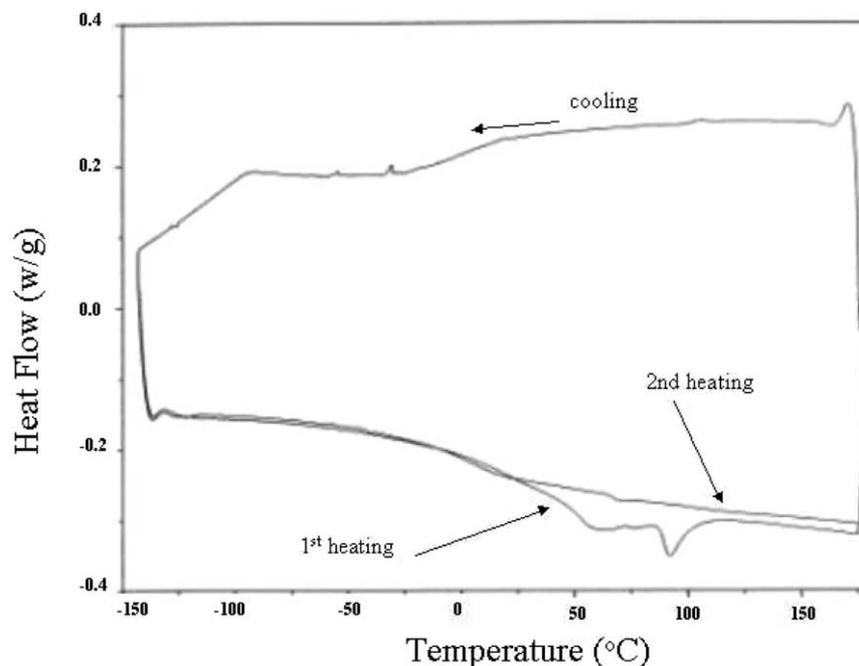

Fig. 2. DSC trace of sample EP70, demonstrating the cold crystallization peaks in the first heating curve (curve closest to the bottom).

sample, leading to a miscible blend continuous phase, compared to a rigid acrylic continuous phase in the case of the SB/LB blends from SANS results. The mechanical properties tend to reflect the film T_g, with higher acrylic content leading to harder films (SB and LB blends). After the QUV-B treatment, the modulus of all samples increases (becomes harder), and this could be induced by the mass loss of lower molecular mass components due to the thermal cycling and UV exposure.

Because it is difficult to use traditional DSC to probe the morphology of these resin blend systems, we have investigated the use of the SANS technique to probe the morphology. Fig. 3 shows SANS results for two fluoropolymer/acrylic coating films having the same composition (F/A=70:30), but prepared by different methods—emulsion polymerization process (EP) versus solution blend (SB). A peak is evident in the intensity profile of the EP70 blend at $q_{peak} = 0.075 \pm 0.002 \text{ nm}^{-1}$ (Peak A), which corresponds to a predominant domain size $d = 84 \pm 2 \text{ nm}$ ($d = 2\pi/q_{peak}$). This d value corresponds roughly to the diameter (D_w in Table 1) of the fluoropolymer seed (latex) particles used to make the EP material (Table 1). For the EP30 material, which had a larger latex particle size (see Table 1), the same peak is observed (Fig. 5) but with a commensurately larger d value ($q_{peak} = 0.052 \pm 0.002 \text{ nm}^{-1}$, $d = 120 \pm 4 \text{ nm}$) compared to EP70. No such structure was observed in the scattering profiles of the solution blend SB70. Peak A is believed to reflect density fluctuations in the film due to incomplete latex film formation, i.e. incomplete diffusion of the resin components across residual particle boundaries to make a truly homogeneous continuous medium. Fig. 4 shows AFM evidence for such structures at the surface of the film—surface corrugation from the residual latex particles can clearly be seen. (This corrugation is also observed in AFM height images, and in SEM micrographs). Peak A may also include contributions from vestiges of any structure ('core-shell' type) that was inherent in the EP latex particles, or from hydrophilic materials such as surfactants. Surfactants have been shown in some cases to pool in the interstices that result from the latex particle packing during film formation [15].

The second peak (Peak B, $d = 15.7 \pm 3 \text{ nm}$), which has a size characteristic of the distance between fluoropolymer crystalline-lamella structures [16], is more pronounced in the solution blend than that in the EP blend. Since the Peak B amplitude for different samples also is commensurate with the amount of crystallinity (first heat enthalpy of melting), as determined by the DSC data (see Table 1), the attribution of this peak to crystalline structures seems compelling.

The SANS data show that there is a higher ordered crystallinity (a well-defined Peak B) in the solution blend (SB) material than in the EP material (a broader Peak B).
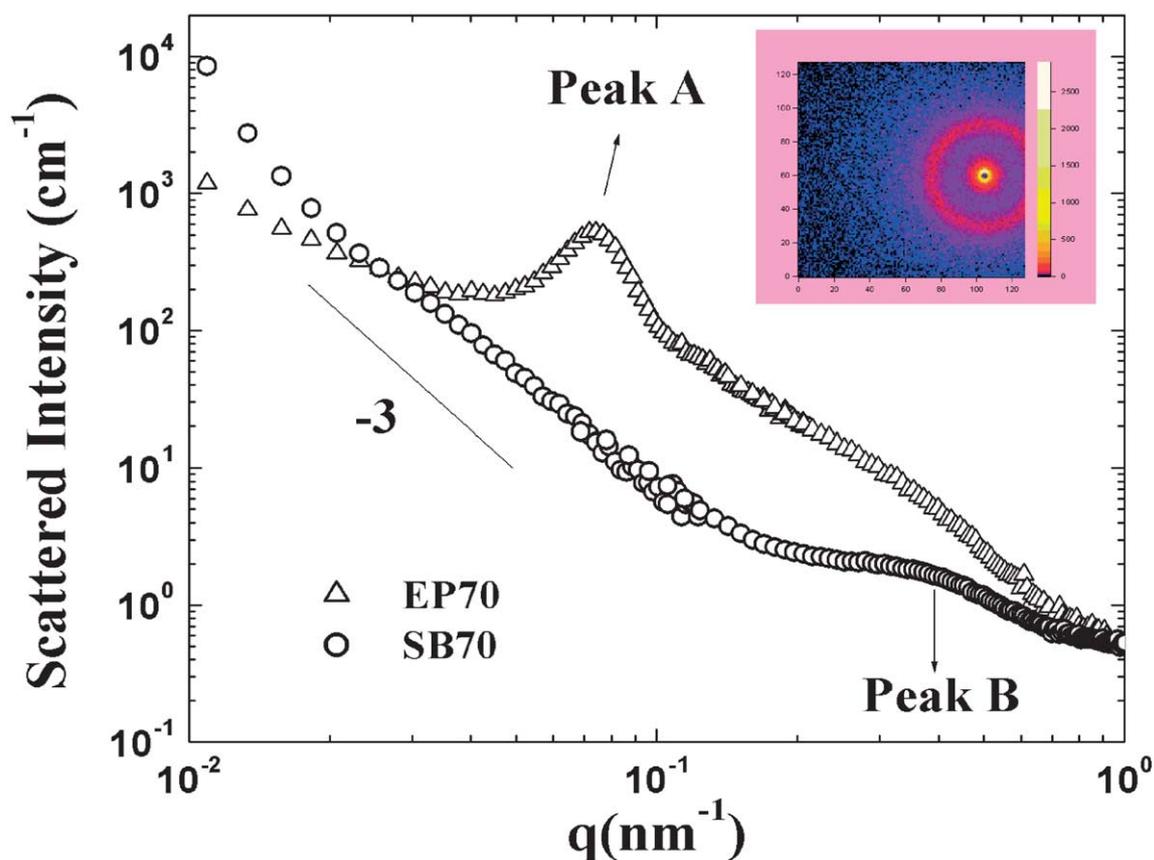

Fig. 3. The scattering intensity as a function of scattering angle of two coatings (F/A=70:30) prepared by emulsion polymerization process (△) and solution blending (○). Insert shows 2D SANS image of the low q section. The estimated extended uncertainties ($k=2$) are smaller than the size of symbols.
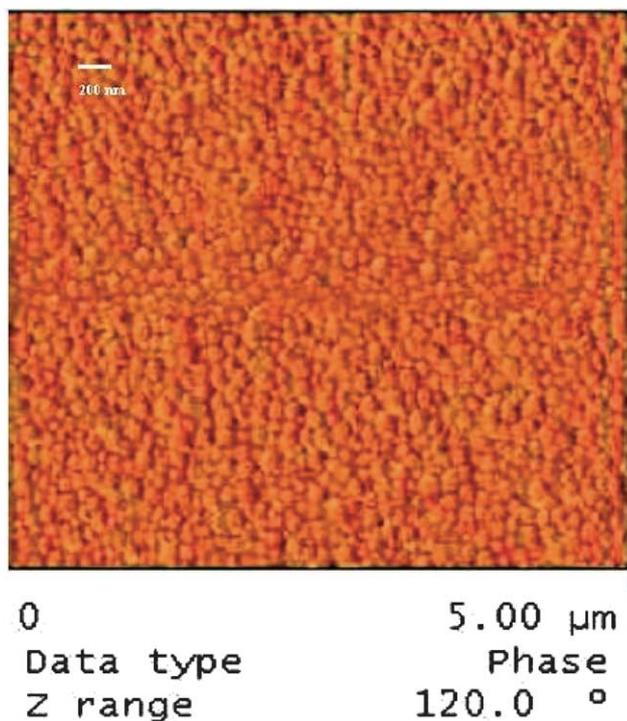
Fig. 4. AFM micrograph of EP70 film (top surface). The residual surface corrugation from the original latex particles can be seen. Image was collected in phase imaging mode, with a scan rate of 1.0 Hz and a set point adjusted to optimize the image.

This implies that the crystallization kinetics were faster than the polymer mixing kinetics in the solution blend, a result consistent with the DSC data (T_g values in Table 1). A higher crystalline fraction means the complementary amorphous phase is enriched in high T_g acrylic. In general, acrylic-enriched regions should also contribute more to the DSC signal, given the heat capacities of the pure polymer components.

For $q < 0.1$ nm^{-1}, the intensity profile of the solution bend follows a q^{-3} scaling law behavior. Note that a $I(q) \sim q^{-4}$ scaling law behavior implies three-dimensional objects with a smooth surface [8]. This q^{-3} scaling law behavior indicates that the interface between the fluoropolymer-rich and acrylic-rich micro-domains was not smooth but diffuse, with a surface fractal dimension of 3 [8]. The higher crystallinity and enhanced large length scale structure would account for the glass transition temperature, T_g, being higher for SB compared to EP samples at the same F/A ratio. This effect would likewise account for differences seen in the tensile mechanical properties, where the films prepared from solution are more rigid (see Tensile Young's modulus values in Table 1).

Fig. 5 shows a comparison of the SANS results for samples EP30, SB30, and LB30, all having an F/A ratio of 30:70. Similar to Peak A in Fig. 3, the EP30 sample has a well-defined peak (Peak A, $d = 114 \pm 3$ nm, larger than the size of fluoropolymer-rich latex in the sample EP70), while the Peak B is not obvious (only a little shoulder in the
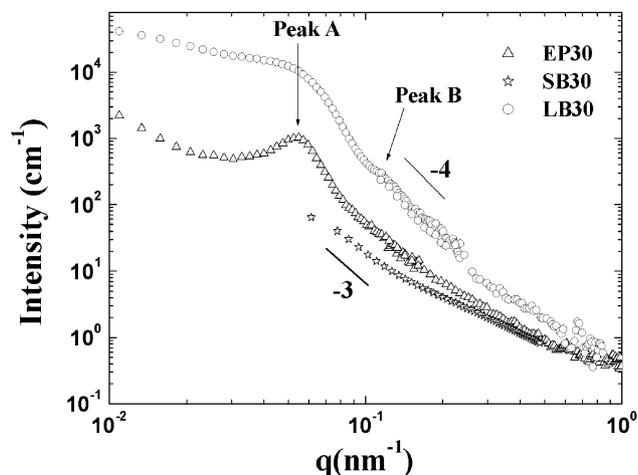

Fig. 5. SANS results for three coatings having same composition (F/A = 30:70) prepared by latex blending, solution blending, and EP techniques.

scattering profile) due to the lower fluoropolymer content (lower crystallinity). We estimated the q_{peak} of Peak B in EP30 data about ~ 0.12 nm^{-1}, which is smaller than that in EP70. This implies the d spacing between fluoropolymer crystalline-lamella structures in EP30 (≈ 52 nm) is larger than that in EP70 (≈ 15.7 nm). The SANS scattering profile of the SB30 blend also follows a q^{-3} scaling law behavior, which is similar to SB70. However, it is hard to define a Peak B feature in SB30 (or else the width of Peak B is very broad).

The scattered intensity of the latex cold blend (LB) sample is much higher than that of the EP film, in the low q region. This result suggests a higher contrast between the two micro-domains (from the original fluoropolymer and acrylic latex particles). The size distribution of fluoropolymer-rich domains in LB samples is broader than that in EP30 since a broader peak is observed.

Moreover, from the $I(q) \sim q^{-4}$ scaling law behavior in the high q region, we can conclude that a sharp interface exists between the fluoropolymer-rich and acrylic-rich micro-domains. Peak B is almost visible in the LB30 profile, and its peak location is similar to that of EP30. It becomes sharper after QUV exposure (see Fig. 6).

From SANS results of the EP coating, it can be observed that:

(1) The length scale associated with Peak A increases with increasing acrylic content.
(2) The distance between neighboring crystalline structures, which is associated with the position of Peak B, increases with increasing acrylic content.

These results are consistent with the latex particle size measurements using CHDF techniques from EP latex solutions, and the ΔH values obtained by DSC measurements listed in Table 1. The CHDF particle size measures hydrodynamic volume, including the electrical double layer, which is typically slightly higher than the actual
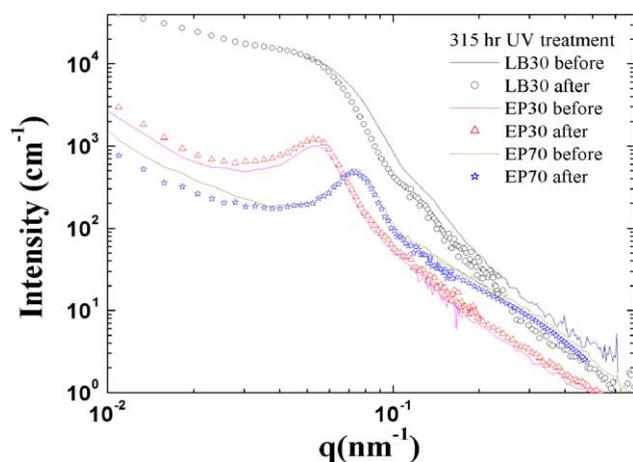
Fig. 6. SANS results for three samples before and after 315 h QUV-B treatment.

polymer particle size. An additional reason for the difference between the CHDF and SANS size measurements is that the CHDF method cannot distinguish the fluoropolymer-core from the acrylic-shell, while the SANS measures the contrast between the fluoropolymer-rich and acrylic-rich micro-domains.

In Fig. 6, the scattering profiles of three coatings after 315 h of UV exposure were presented for the water borne systems (LB and EP). Overall, exposure-induced changes in the scattering profile of the EP coatings are not noticeable (both EP30, EP70), especially for the position and width of Peak A. This implies that the microstructure of EP films is unchanged after the UV exposure. On the other hand, exposure-induced changes are seen for LB30 with the second peak (Peak B) becoming more evident. This could be due to local rearrangements of the crystalline structures, consistent with the observed increase in the crystallinity fraction (ΔH) data after UV treatment (in Table 1). Similar results have been observed for different PVDF-based coating systems using AFM techniques [16].

The results obtained from SANS are consistent with the UV induced mass loss results shown in Fig. 1. The in situ EP blends preserve the microstructure/morphology and show more robust durability performance (QUV-B treatment) than the LB (physically mixed) blends. This result is also consistent with the results of earlier annealing experiments, reported in Ref. [5], in which films made from fluoropolymer core-acrylic shell latex particles were annealed at progressively higher temperatures. In that study, the QUV mass loss, and the gloss retention, improved dramatically for films annealed at temperatures at or above the fluoropolymer crystalline melting temperature, where the miscible polymers could interdiffuse.

4. Concluding remarks

SANS results provide morphology/microstructure information on blends prepared by different mixing methods. It is evident that during film formation, coatings prepared by an emulsion polymerization (EP) process preserve their microstructure/morphology, and show more robust QUV-B exposure performance compared to coatings made from blends of single polymer latexes (LB). Although a single T_g is observed in all cases, EP blends were found to be softer and more elastic than LB and SB blends. Because several factors affect the mechanical properties, it will be difficult to assess exactly where these differences come from. However, likely important factors include the less homogeneous degree of mixing in the LB blends, and different blend morphologies for the more intimately mixed EP and SB blends.

During QUV-B exposure, all samples underwent changes in physical and mechanical properties that are mainly attributable to acrylic polymer degradation, as well as possibly the leaching of formulation co-solvents, and low molecular mass species from the acrylic polymerization process. However, these changes were much more pronounced in the case of LB blends. Again, the higher degree of mixing in EP blends seems to allow for a better protection of the acrylic polymer, hence a longer weatherability.

This work showed that it is necessary to consider many factors in evaluating the mechanical properties and the weatherability of fluoropolymer/acrylic mixtures, such as the ratio between the two components, the acrylic fraction, the level of blending, and the compatibility between the two components and between the amorphous and crystalline phases.

References

[1] Iezzi RA. Fluoropolymer coatings for architectural application Modern fluoropolymer. New York: Wiley; 1997. Chapter 14, pp. 271.
[2] Scheirs J, Burks S, Locaspi A. TRIP (Trends in Poly Sci) 1995;3:74.
[3] Iezzi RA, Gaboury S, Wood A. Prog Org Coat 2000;40:55.
[4] Bernstein RE, Crua CA, Paul DR, Barlow JW. Macromolecules 1977; 10:681.
[5] Wood KA, Cypcar C, Hedhli L. J Fluorine Chem 2000;104:63.
[6] Hare CH. Protective Coatings, the Fundamentals of Chemistry and Composition. Pittsburgh, PA: Technology Publishing Company; 1994.
[7] Choi SM, Barker JG, Glinka CJ, Cheng YT, Gammel PL. J Appl Cryst 2000;33:793.

[8] Higgins JS, Benoit HC. Polymers and neutron scattering. Oxford, UK: Clarendon Press; 1994.

[9] ASTM G53-88 Standard Practices for Operating Light and Water Exposure Apparatus (Fluorescence UV-Condensation Type) for Exposure of Nonmetallic Materials. American Society for Testing and Materials: West Conshohocken, PA, USA.

[10] ASTM D823-95 Standard Practices for Producing Films of Uniform Thickness of Paint, Varnish, and Related Products on Test Panels. American Society for Testing and Materials: West Conshohocken, PA, USA.

[11] Wood KA, Hedhli L, Willcox J. PMSE Preprint 2000;76:148.

[12] Vicini S. PhD Thesis, University of Genoa, 2002, unpublished results.

[13] Fox TG. Bull Am Phys Soc 1956;1:12. Fox equation for calculating T_g for a 2-component polymer blend: $(T_g)^{-1} = m_1(T_{g,1})^{-1} + m_2(T_{g,2})^{-1}$, where m_1 and m_2 are the mass fractions of each polymer in the blend; $T_{g,1}$ and $T_{g,2}$ are their glass transition temperatures respectively. See Fox TG. Bull Am Phys Soc, 1956;1:12.

[14] Ando Y, Hanada T, Saito K. J Polym Sci, Part B: Polym Phys 1994; 32:179.

[15] Bueckmann AJP, Overbeek GC, Nabuurs T. Paint and coatings industry 2001 pp. 40.

[16] Gu X, Sung L, Ho DL, Michaels CA, Nguyen D, Jean YC, Nguyen T. FSCT ICE 2000 Proceedings of the 80th Annual meeting technical program, New Orleans, LA 2002.